



Published in final edited form as:

*Addict Biol.* 2023 January ; 28(1): e13258. doi:10.1111/adb.13258.

## Evaluating Instrumental Learning and Striatal-cortical Functional Connectivity in Adolescent Alcohol and Cannabis Use

NA Hubbard<sup>1,\*</sup>, KB Miller<sup>1</sup>, J Aloï<sup>2</sup>, S Bajaj<sup>3</sup>, KT Wakabayashi<sup>1</sup>, RJR Blair<sup>4</sup>

<sup>1</sup>Department of Psychology, University of Nebraska-Lincoln, Lincoln, NE

<sup>2</sup>Department of Psychiatry, Indiana University School of Medicine, Indianapolis, IN

<sup>3</sup>Center for Neurobehavioral Research in Children, Boys Town National Research Hospital, Boys Town, NE

<sup>4</sup>Child and Adolescent Mental Health Centre, Mental Health Services, Capital Region of Denmark, Copenhagen, Denmark

### Abstract

Adolescence is a vulnerable time for the acquisition of substance use disorders, potentially relating to ongoing development of neural circuits supporting instrumental learning. Striatal-cortical circuits undergo dynamic changes during instrumental learning and are implicated in contemporary addiction theory. Human studies have not yet investigated these dynamic changes in relation to adolescent substance use. Here, functional magnetic resonance imaging was used while 135 adolescents without (AUD-CUD<sub>Low</sub>) and with significant alcohol- (AUD<sub>High</sub>) or cannabis-use-disorder symptoms (CUD<sub>High</sub>) performed an instrumental learning task. We assessed how cumulative experience with instrumental cues altered cue-selection preferences and functional connectivity strength between reward-sensitive striatal and cortical regions. Adolescents in AUD<sub>High</sub> and CUD<sub>High</sub> groups were slower in learning to select optimal instrumental cues relative to AUD-CUD<sub>Low</sub> adolescents. The relatively fast learning observed for AUD-CUD<sub>Low</sub> adolescents coincided with stronger functional connectivity between striatal and frontoparietal regions during early relative to later periods of task experience, whereas the slower learning for the CUD<sub>High</sub> group coincided with the opposite pattern. The AUD<sub>High</sub> group not only exhibited slower learning, but also produced more instrumental choice errors relative to AUD-CUD<sub>Low</sub> adolescents. For the AUD<sub>High</sub> group, Bayesian analyses evidenced moderate support for *no* experience-related changes in striatal-frontoparietal connectivity strength during the task. Findings suggest that adolescent cannabis use is related to slowed instrumental learning and delays in peak functional connectivity strength between the striatal-frontoparietal regions that support this learning, whereas adolescent

\* To whom correspondence may be addressed: Nicholas A. Hubbard, University of Nebraska-Lincoln, Center for Brain, Biology, and Behavior, C82 East Stadium, Lincoln, NE 68588, nhubbard5@unl.edu.

**Author Contributions:** NAH performed analysis and drafted the manuscript. KBM performed analysis and drafted the manuscript. JA, SB, and KTW contributed critical revisions to the manuscript and aided in interpretation. RJRB drafted the manuscript and was responsible for the study concept and design.

**Disclosures:** The authors do not declare any known conflicts of interest related to this work.

**Data Availability:** The data that support the findings of this study are available from the corresponding author upon reasonable request.

alcohol use may be more closely linked to broader impairments in instrumental learning and a general depression of the neural circuits supporting it.

### Keywords

ADOLESCENCE; ALCOHOL; CANNABIS; FUNCTIONAL MAGNETIC RESONANCE IMAGING; INSTRUMENTAL LEARNING

Alcohol and cannabis use disorders are the most prevalent substance disorders afflicting US adolescents.<sup>1</sup> Considerable effort has been devoted to examining reward-related processes in striatal basal ganglia associated with adolescent alcohol and cannabis use.<sup>2–6</sup> The striatum and broader basal ganglia have established roles in reward processing and instrumental learning<sup>7,8</sup>—the strengthening of associations among predictive cues, actions, and outcomes which impact the likelihood of reproducing actions. Striatal function and instrumental learning also have implications for understanding and treating substance use disorders.<sup>9–12</sup> For instance, several behavioral therapies for substance-use disorders capitalize upon instrumental learning to promote abstinence (e.g., motivational enhancement, contingency management).<sup>12</sup> Importantly, striatal regions are thought to function in concert with a network of cortical regions when influencing both instrumental learning<sup>13</sup> and addictive behaviors.<sup>11</sup> Yet, there is no evidence available from human developmental research indicating how functional relationships between the striatum and cortex may relate to altered instrumental learning associated with substance use.

Adolescent alcohol and cannabis use are associated with alterations in striatal and frontoparietal (i.e., dorsolateral prefrontal cortex [dlPFC] and parietal cortex) functions, which may have implications for instrumental learning.<sup>13</sup> Indeed, adolescent alcohol and cannabis use have been linked to performance deficits on tasks that permit learning through reward and punishment feedback.<sup>14,15</sup> Functional magnetic resonance imaging (fMRI) studies have also demonstrated altered activations in striatum during tasks that feature reward and punishment events associated with adolescent alcohol or cannabis use.<sup>2–6</sup> For example, adolescents who binge-drink show decreased striatal activation during reward anticipation, relative to non-binge-drinking adolescents<sup>6</sup> and greater adolescent cannabis-use-disorder symptoms are related to decreased striatal activations during punishment feedback.<sup>2</sup> Regarding frontoparietal regions, fMRI findings have indicated reduced representation of reward prediction error (RPE) and expected value signals (covert factors of reinforcement-learning models) by brain activations in these regions during instrumental learning associated with adolescent alcohol and/or cannabis use.<sup>4,15</sup> A recent meta-analysis has also indicated that substance use more broadly is characterized by reduced representation of a range of prediction-error signals (covert factors of learning) in both striatal and lateral prefrontal regions.<sup>16</sup>

To our knowledge, only one study has examined functional relationships among striatal and cortical regions during instrumental learning in the context of substance use.<sup>17</sup> There, adults with alcohol use disorder demonstrated weaker functional connectivity between ventral striatal and dlPFC regions during an instrumental learning task, as well as behavior consistent with slower learning of instrumental contingencies (i.e., cue-action-outcome

associations) relative to adults without this disorder. These findings highlighted possible links amongst adult substance use, striatal-frontoparietal functional connectivity, and slowed instrumental learning. It is not known, however, whether adolescent substance use is related to altered striatal-frontoparietal functional connectivity during instrumental learning. Further, no study has characterized how striatal-frontoparietal functional connectivity changes over the course of adolescents' instrumental learning or whether such experience-related changes in functional connectivity might be altered in the context of substance use. Yet, examining experience-related changes is critical for investigating the neural correlates of learning, as functional connections among striatal and cortical regions evolve as participants gain experience and become more proficient in performing instrumental learning tasks.<sup>18</sup>

The present study addressed these gaps by examining how adolescents' functional connectivity between striatum and frontoparietal regions changed with cumulative experience on an instrumental learning task, and whether potential impairments in learning for adolescents with significant alcohol- (AUD<sub>High</sub>) or cannabis-use-disorder symptoms (CUD<sub>High</sub>) coincided with altered functional connectivity between these regions. Instrumental learning was examined using a passive avoidance task (PAT). This task is sensitive to performance deficits associated with adolescent alcohol and/or cannabis use and has demonstrated reduced representation of RPE and expected-value signals in striatal and frontoparietal regions related to adolescent use of these substances.<sup>15</sup> Consistent with the slower learning of instrumental contingencies observed in an adult substance use disorder,<sup>17</sup> we first predicted that adolescents in the AUD<sub>High</sub> and CUD<sub>High</sub> groups would exhibit a slower rate of decline in instrumental choice errors over the course of the PAT, relative to adolescents not presenting with these symptoms (AUD-CUD<sub>Low</sub>). Instrumental choice errors were defined as failures to choose cues associated with high reward probabilities and failures to avoid choosing cues associated with high punishment probabilities.<sup>4,18,15</sup> We examined these errors because they encompassed instrumental learning in the context of both positive reinforcement and negative punishment contingencies.

Second, we examined whether experience on the PAT differentially altered AUD<sub>High</sub> and CUD<sub>High</sub> adolescents' functional connectivity between striatum and frontoparietal regions, relative to adolescents in the AUD-CUD<sub>Low</sub> group. Experience effects were investigated by examining changes in functional connectivity strength across the first and second halves of the PAT (i.e., early- and late-experience phases).<sup>19</sup> Coordinated activation among basal ganglia and, task-relevant prefrontal and posterior cortical regions is hypothesized to support the initial learning of instrumental contingencies.<sup>20</sup> However, after contingencies are sufficiently learned through experience, coordinated activation among basal ganglia and these cortical regions may no longer be needed to support instrumental behaviors.<sup>20</sup> Consistent with this hypothesis, we predicted that relatively fast learning of instrumental contingencies by adolescents in the AUD-CUD<sub>Low</sub> group would be accompanied by strong functional connectivity (our operationalized measure of coordinated activity) between reward-sensitive striatum and frontoparietal regions during the early-experience phase of the PAT, followed by a decrease in strength during the late-experience phase. For adolescents in the AUD<sub>High</sub> and CUD<sub>High</sub> groups, however, we predicted that slower learning of instrumental contingencies would be accompanied by a relative delay in peak striatal-

frontoparietal connectivity strength. Specifically, we predicted functional connectivity among these regions may be relatively weak during the early-experience phase and increase for the late phase of the PAT. Alternatively, it is possible that compromised learning in these groups may be accompanied by minimal experience-related changes in striatal-frontoparietal connectivity strength.

## Method

### Participants and Procedure

This article presents novel tests of behavioral and neural predictions using previously described data.<sup>3</sup> Adolescents (ages 14 to 18 years) were recruited from a residential treatment program and the surrounding Omaha, Nebraska community as part of a broader study examining youth behavioral and emotional problems (including substance use).<sup>21,2,3</sup> Procedures were approved by the Boys Town National Research Hospital Institutional Review Board. Parental informed consent and adolescent assent was obtained. Exclusion criteria: scores on the Wechsler Abbreviated Scale of Intelligence Full-scale IQ < 75 (FS-IQ)<sup>22</sup> pregnancy; non-psychiatric conditions requiring the use of medication with potential psychoactive effects (e.g., beta blockers, steroids); current psychosis; pervasive developmental disorders; Tourette's disorder; neurological disorders; metallic objects in the body; and claustrophobia. Current psychiatric conditions (other than psychotic disorders or pervasive developmental disorders) and medication for psychiatric conditions were not exclusionary. Participants taking stimulant medication were asked to withhold use of this medication on the day of scanning. Psychiatric diagnoses were established via clinical interview of adolescents and their parents/caregivers administered by licensed and board-certified child and adolescent psychiatrists. Diagnoses were assigned according to DSM-V criteria.

Structural and functional magnetic resonance imaging (MRI) data were available from 142 participants. Data were retained for 135 adolescents after quality assurance procedures, wherein: one dataset was discarded due to failed functional-structural registration, four datasets were discarded due to duplicate fMRI sessions (e.g., participant needed to restart task), and two datasets were discarded due to missing PAT behavioral data.

### Characterization of Alcohol and Cannabis Use

Adolescent alcohol- and cannabis-use-disorder symptoms were characterized via the Alcohol Use Disorder Identification Test (AUDIT)<sup>23</sup> and Cannabis Use Disorder Identification Test (CUDIT)<sup>24</sup>. These assessed the quantity and frequency of alcohol or cannabis use, as well as the psychosocial consequences experienced due to use in the past 1 year or 6 months. AUD<sub>High</sub> status was characterized using the alcohol-use-disorder clinical threshold suggested for the AUDIT ( < 4)<sup>25</sup>. CUD<sub>High</sub> status was characterized using the cannabis-use-disorder clinical threshold suggested for the CUDIT ( < 8)<sup>24</sup>. Group characterization was based solely upon AUDIT and CUDIT scores, not clinical diagnoses. Approximately 24% (32/135) of participants reached both AUDIT and CUDIT thresholds, these participants were included in analyses for both AUD<sub>High</sub> and CUD<sub>High</sub> groups.

Adolescents failing to reach thresholds on both the AUDIT and CUDIT were assigned to the control group (AUD-CUD<sub>Low</sub>).

### Passive Avoidance Task (PAT)

The PAT is an fMRI-adapted instrumental learning paradigm presenting cues that, if acted upon, offer a chance to win or lose virtual money (see Figure 1A)<sup>3,15</sup>. One of four cue shapes was presented per trial (1500 ms). Participants chose whether to respond to the cue. The cue was then removed, and a fixation period occurred (jittered: 0–4000 ms). If participants chose not to respond to the cue, a blank screen was presented (1500 ms). If they chose to respond, feedback was presented informing them that their choice resulted in winning or losing money (1500 ms). Feedback followed a probabilistic reinforcement schedule: two shapes (high reward probability cues) were associated with an 80% chance of a reward (+\$1 or +\$5), and a 20% chance of punishment (-\$1 or -\$5); and two shapes (high punishment probability cues) were associated with an 80% chance of a punishment (-\$1 or -\$5), and a 20% chance of reward (+\$1 or +\$5). After choice-feedback or the no-choice blank screens, a fixation period preceded a subsequent trial (jittered: 0–4000 ms).

A brief practice PAT was administered outside of the scanner to familiarize participants with performing a PAT. The practice PAT utilized different cues and reinforcement schedules than the actual PAT (see Supporting Information). During the actual PAT, responses were registered via button boxes. Four cue types were presented 27 times each, in random order (108 total trials). The target behavioral measure was instrumental choice errors, which indexed a failure to choose a cue associated with high reward probability or a failure to avoid choosing a cue associated with high punishment probability.<sup>4,18,15</sup>

### Image Acquisition and Processing

**Acquisition.**—Images were acquired from a Siemens 3-Tesla MAGNETOM Skyra MRI scanner with a 20-channel head coil. A T1-weighted magnetization-prepared rapid gradient echo (MPRAGE) sequence acquired whole-brain (176 axial slices), high-resolution anatomical images using the following parameters: TR=2200 ms, TE=2.48 ms, FoV=200 mm, Flip Angle=8°, 256×208 matrix, 0.9×0.9×1 mm<sup>3</sup> voxel size. A T2\*-weighted gradient-recalled echo planar imaging sequence acquired whole-brain (43 axial slices) blood-oxygen-level dependent (BOLD) signals during the PAT task using the following parameters: TR=2500 ms, TE=27 ms, FoV=240 mm, Flip Angle=90°, 94×94 matrix, 2.6×2.6×2.5 mm<sup>3</sup> voxel size.

**Processing.**—Images were preprocessed using a standardized *fmrprep* processing workflow (v.20.2.1) including: T1w bias-field correction, brain extraction, normalization to the ICBM-152 Nonlinear Asymmetrical template, compartmental segmentation, and motion correction and quantification procedures.<sup>26</sup> Preprocessed functional volumes were spatially smoothed (6 mm Gaussian kernel). Motion outliers were defined via a Euclidean-norm approach with a head-displacement threshold comparable to previous youth fMRI studies (.7 mm)<sup>27,28</sup>. An a priori threshold was set to discard a participant's data if 20% or more of their functional volumes were deemed motion outliers<sup>29</sup>; this threshold excluded zero participants. Analysis of Functional Neuroimages (AFNI) software<sup>31</sup> was used to build

generalized linear models (GLMs) estimating BOLD activations during the PAT while: (1) controlling for three translation and three rotation head-motion estimates and frame-wise displacement<sup>30</sup>; (2) employing an automatic polynomial (high-pass) filter to minimize additional temporal trends (e.g., signal drift); and (3) preventing the volumes deemed motion outliers (see above) from influencing the GLM output (via *3dDeconvolve -censor*).

**Localization of Reward-sensitive Nodes.**—Striatal and cortical regions differentially responsive to PAT instrumental contingencies were localized functionally. BOLD time series and stimulus timings for high reward and high punishment probability cues were convolved with double-gamma impulse response functions using the aforementioned GLM procedures. Beta weights were aggregated across all participants and subjected to a sample-wide, whole-brain *t*-test contrasting weights derived from high reward and high punishment probability cues ( $\text{High}_{\text{Reward}} > \text{High}_{\text{Punish}}$ ). Clusters of significant activation ( $z = 3.94$ ; *k*-faces-touching voxels  $> 49$ ; *FWER*-corrected  $p < .001$ ) were transformed into 13, non-overlapping nodes of equal volume via a 7 mm sphere placed at each cluster's peak voxel<sup>28</sup>; hereafter, described as reward-sensitive nodes. These nodes were used in subsequent analyses.

**Functional Connectivity between Reward-sensitive Nodes.**—Analyses evaluated functional connectivity strength between the reward-sensitive striatal node ( $\text{RS}_{\text{Striatum}}$ ) and the remaining 12 reward-sensitive nodes across the early and later experience phases of the PAT. The first 54 trials were operationalized as the early experience phase, the last 54 trials comprised the late phase.<sup>19</sup> For the entire sample, the averaged rate of change in choice error probabilities (see Statistical Analysis below) reached an approximate asymptote during the early phase, indicating instrumental choice performance approached an approximate steady state for many adolescents by the late phase (Figure 1B–C). Equal division of trials was necessary to ensure similar statistical power was afforded to both experience phase conditions.

Trial-by-trial BOLD activations during early- and late-experience phases for  $\text{High}_{\text{Reward}}$  and  $\text{High}_{\text{Punish}}$  cues were modeled as separate regressors via convolution with double-gamma impulse response functions using the aforementioned GLM procedures (see also Supporting Information). Beta weights for each trial of these four conditions were averaged spatially across voxels within each reward-sensitive node, providing a single beta-series per node.<sup>27</sup> Pearson correlations were computed using these beta-series between  $\text{RS}_{\text{Striatum}}$  and the remaining 12 reward-sensitive nodes, producing functional connectivity coefficients with  $\text{RS}_{\text{Striatum}}$  for all four conditions.<sup>32</sup> This approach produced a connectivity matrix for each condition (four conditions total) from which functional connectivity strength with  $\text{RS}_{\text{Striatum}}$  could be examined.

Bidirectional functional connectivity strength with  $\text{RS}_{\text{Striatum}}$  was computed on each of the four matrices using Brain Connectivity Toolbox.<sup>33</sup> We did not have specific hypotheses regarding functional connections between the striatum and individual reward-sensitive frontoparietal nodes, as lateral DLPFC and parietal regions are implicated in shared cognitive processes during reinforcement learning.<sup>13</sup> Therefore, the strength of functional connections with  $\text{RS}_{\text{Striatum}}$  was calculated amongst the positive connections aggregated across the four reward-sensitive frontoparietal nodes to limit family-wise error and aid

in interpretations (hereafter,  $RS_{FP}$  nodes)<sup>27</sup>. This same procedure was performed to estimate the strength of functional connectivity between  $RS_{Striatum}$  and all other reward-sensitive nodes excluding the frontoparietal nodes (hereafter,  $RS_{Other}$  nodes). See Supporting Information for expanded description.

## Statistical Analyses

**Substance-use-disorder Groups and Dimensions.**—We tested whether  $AUD_{High}$  and  $CUD_{High}$  groups differed from the  $AUD-CUD_{Low}$  group on instrumental choice behaviors and functional connectivity. For functional connectivity analyses, AUDIT and CUDIT scores were additionally rankit transformed and z-standardized<sup>2–4</sup> providing a dimensional covariate to investigate the specificity of substance-use-disorder-group effects. That is, for significant group-level effects (e.g.,  $CUD_{High}$  versus  $AUD-CUD_{Low}$  status), the extent of participants' symptoms related to the other substance (e.g.,  $zAUDIT$  score) were covaried to examine whether effects were specific to a particular form of substance-use-disorder symptomology. This approach was used in lieu of directly comparing  $AUD_{High}$  versus  $CUD_{High}$  groups because of non-exclusivity and co-use between these groups. The continuous measures also allowed us to evaluate specific dimensional effects of alcohol- or cannabis-use-disorder symptoms on functional connectivity. Combined results from  $AUD_{High}$  and  $CUD_{High}$  versus  $AUD-CUD_{Low}$  status are provided in Supporting Information.

**Instrumental Learning Rate.**—Instrumental choice errors were obtained from each PAT trial for each participant. Instrumental choice error probabilities were used for group-level tests and were calculated as the proportion of group members committing an instrumental choice error on each trial. Instrumental learning rates were investigated using a single-term, power series regression (Figure 1B–C), consistent with power-law relationships observed between task experience and associative learning/memory performance.<sup>34,35</sup> Power-series regression models estimated the decrease of instrumental choice error probabilities with accumulating experience on the PAT. More negative decay rate parameters ( $x^b$ ) were operationalized to reflect faster learning of instrumental contingencies.

Between-groups effects on learning rate were assessed using bootstrap aggregation to generate unbiased distributions of  $x^b$  parameters. Therein, group members were randomly resampled with replacement and a new power-series model was fit to the resampled instrumental choice error probabilities ( $B=5000$ ). One-tailed, percentile bootstrap tests examined overlap between the original  $x^b$  parameter estimates for each group and the *upper*-bound of the 95% confidence limit derived from the bootstrap  $x^b$  parameter distribution of the non-dependent group ( $AUD-CUD_{Low}$ ). The same approach was used to test whether the original  $x^b$  parameter estimate for the  $AUD-CUD_{Low}$  group surpassed the *lower*-bound of the 95% confidence limit derived from bootstrap  $x^b$  parameter distributions from the substance-use-disorder groups.

**Overall Instrumental Choice Errors.**—Mann-Whitney  $U$ -tests were used to examine between-group differences in the average probability of an instrumental choice error across all trials of the PAT. Rank-biserial correlations ( $r_{rb}$ ) provided effect sizes. Non-parametric tests were chosen because average choice error probabilities were non-normally distributed.

**Experience-related Functional Connectivity Changes.**—Repeated-measures ANOVAs tested Experience Phase (Early, Late), Cue (High<sub>Reward</sub>, High<sub>Punish</sub>), and substance-use-disorder Group effects on functional connectivity strength. Primary hypothesis tests examined whether group status was related to differential changes in the strength of functional connectivity between RS<sub>Striatum</sub> and RS<sub>FP</sub> nodes across experience phases (i.e., Experience Phase × Group interactions). Additional repeated-measures ANOVA models were used to rule-out broader functional connectivity effects by examining functional connections between RS<sub>Striatum</sub> and RS<sub>Other</sub> nodes<sup>27</sup>.

**Potential Confounding Factors.**—Covariates were examined to assess whether their inclusion into the repeated-measures ANOVA influenced the significance of Experience Phase × Group effects. Demographic/clinical covariates included: Age, binary Sex, FS-IQ (Wechsler Abbreviated Scale of Intelligence Full-scale IQ)<sup>22</sup>, In-Patient Status (i.e., in-patient vs. community-dwelling), the absence or presence of any non-substance-dependence DSM-5 diagnosis (Any Diagnosis), and the current use of any psychiatric medication (Any Medication) were tested as covariates. DSM-5 Diagnoses with a sample-wide incidence of at least 20 cases were also evaluated: ADHD ( $n = 69$ ), Conduct Disorder ( $n = 61$ ), Generalized Anxiety Disorder ( $n = 36$ ), Oppositional Defiant Disorder ( $n = 73$ ), and Social Anxiety Disorder ( $n = 28$ ). The same criterion was used for psychiatric medications, including: Antidepressants ( $n = 25$ ) and Stimulants ( $n = 20$ ). The influence of cigarette smoking (ranging from 0 [never] to 4 [current, regular use]) obtained from the Monitoring the Future Survey<sup>36</sup> was also tested. Imaging-related covariates included head motion estimates via the average framewise displacement values after motion censoring<sup>27</sup>, the number of motion censored frames, averaged BOLD activation changes in RS<sub>Striatum</sub> and RS<sub>FP</sub> across PAT phases in response to High<sub>Reward</sub> and High<sub>Punishment</sub>. Changes in functional connectivity strength between RS<sub>Striatum</sub> and RS<sub>Other</sub> nodes for High<sub>Reward</sub> and High<sub>Punishment</sub> cues across PAT Phases were also tested as covariates to evaluate potential broader effects of RS<sub>Striatum</sub> functional connectivity changes.<sup>27,28</sup>

## Results

### Group Characteristics.

Demographic, clinical, and other characteristics of the retained sample ( $N = 135$ ) may be found in Table 1. Statistical tests contrasting group characteristics may be found in Supporting Tables 1–2.

### Instrumental Learning Rate.

Parametric 95% confidence intervals for each group's  $x^b$  parameter estimate did not contain zero, indicating significant power-law relationships characterizing task experience and instrumental choice error probabilities ( $p < .05$ ; Figure 2A). AUD<sub>High</sub> and CUD<sub>High</sub> groups'  $x^b$  parameter estimates were less negative and did not surpass the upper-bound of the 95% bootstrap confidence limit of the AUD-CUD<sub>Low</sub> group (Figure 2B). The AUD-CUD<sub>Low</sub> group's  $x^b$  parameter was more negative and did not surpass the lower-bound of the 95% bootstrap confidence limits of the AUD<sub>High</sub> and CUD<sub>High</sub> groups (Figure 2B). In sum, all groups demonstrated significant power-law relationships between task experience



and instrumental choice error probabilities, and AUD<sub>High</sub> and CUD<sub>High</sub> groups exhibited significantly slower declines in these errors relative to the AUD-CUD<sub>Low</sub> group.

### Overall Instrumental Choice Errors.

Between-groups analyses failed to indicate a significant difference between CUD<sub>High</sub> and AUD-CUD<sub>Low</sub> groups on the average probability of choice errors,  $W = 1708.00$ ,  $p = .118$ ,  $r_{fb} = -.161$ . However, a significant difference was observed between AUD<sub>High</sub> compared to AUD-CUD<sub>Low</sub> groups, indicating greater average choice error probabilities for the AUD<sub>High</sub> group,  $W = 1003.00$ ,  $p = .029$ ,  $r_{fb} = -.255$  (also see Supporting Information).

### Localization of Reward-sensitive Nodes.

Figure 3A illustrates voxel clusters with significant High<sub>Reward</sub> > High<sub>Punish</sub> activation ( $z = 3.94$ ;  $k$ -faces-touching voxels > 49;  $FWER$ -corrected  $p < .001$ ). Figure 3B illustrates the 13 non-overlapping reward-sensitive nodes (see Table 2).

### CUD<sub>High</sub> and Experience Effects on Functional Connectivity.

A repeated-measures ANOVA using CUD<sub>High</sub> versus AUD-CUD<sub>Low</sub> as the Group factor demonstrated a significant Experience Phase  $\times$  Group interaction effect on functional connectivity strength between RS<sub>Striatum</sub> and RS<sub>FP</sub> nodes,  $F(1,126) = 12.50$ ,  $p < .001$ ,  $\eta_p^2 = .090$  (Figure 4A). The significant Experience Phase  $\times$  Group interaction effect was retained after including  $z$ AUDIT score into the model,  $F(1,125) = 14.20$ ,  $p < .001$ ,  $\eta_p^2 = .102$ —indicating CUD<sub>High</sub> effects remained significant independent of alcohol-use-disorder symptoms. None of the 22 covariates altered the significance of the Experience Phase  $\times$  Group interaction effect on functional connectivity strength between RS<sub>Striatum</sub> and RS<sub>FP</sub> nodes (Effect Range:  $\eta_p^2 = .031 - .135$ ,  $p = <.001 - .048$ ). Simple main effects analyses of Group confirmed that both the AUD-CUD<sub>Low</sub> ( $F(1,126) = 5.23$ ,  $p = .025$ ) and CUD<sub>High</sub> ( $F(1,126) = 6.96$ ,  $p = .011$ ) groups exhibited significant Experience Phase-related changes in functional connectivity strength between RS<sub>Striatum</sub> and RS<sub>FP</sub> nodes, albeit, with opposite directionality. As predicted, the AUD-CUD<sub>Low</sub> group's functional connectivity was significantly stronger during the Early relative to Late Experience Phase, whereas the CUD<sub>High</sub> group's functional connectivity was significantly stronger during the Late relative to Early Experience Phase (Figure 4A).

We failed to observe a significant Experience Phase  $\times$  Group interaction effect on functional connectivity strength between RS<sub>Striatum</sub> and RS<sub>Other</sub> nodes,  $F(1,126) = .004$ ,  $p = .952$ ,  $\eta_p^2 < .001$ . Analyses of simple main effects also failed to find significant Experience Phase-related changes in functional connectivity strength between RS<sub>Striatum</sub> and RS<sub>Other</sub> nodes for either group ( $ps > .05$ ).

### AUD<sub>High</sub> and Experience Effects on Functional Connectivity.

A repeated-measures ANOVA using AUD<sub>High</sub> versus AUD-CUD<sub>Low</sub> as the Group factor demonstrated a trending, but non-significant, Experience Phase  $\times$  Group interaction effect on functional connectivity strength between RS<sub>Striatum</sub> and RS<sub>FP</sub> nodes,  $F(1,106) = 3.69$ ,  $p = .057$ ,  $\eta_p^2 = .034$  (Figure 4B). However, in contrast to all other groups, analyses of simple

main effects for AUD<sub>High</sub> failed to indicate significant Experience Phase-related changes in functional connectivity strength between RS<sub>Striatum</sub> and RS<sub>FP</sub> ( $p > .05$ ; see Supporting Information for Bayesian analyses). Additionally, no significant Experience Phase  $\times$  Group interaction effect was observed on functional connectivity strength between RS<sub>Striatum</sub> and RS<sub>Other</sub> nodes,  $F(1,106) = .014$ ,  $p = .907$ ,  $\eta_p^2 < .001$ . Analyses of simple main effects for AUD<sub>High</sub> failed to find significant Phase-related changes in functional connectivity strength between RS<sub>Striatum</sub> and RS<sub>Other</sub> nodes ( $p > .05$ ).

### Symptom Dimensions and Experience Effects on Functional Connectivity.

An Experience Phase  $\times$  Cue repeated measures ANCOVA was constructed with zAUDIT and zCUDIT scores as covariates to explore dimensional effects of alcohol- or cannabis-use-disorder symptoms. Similar to group-level results, a significant Experience Phase  $\times$  zCUDIT score interaction was observed on functional connectivity strength between RS<sub>Striatum</sub> and RS<sub>FP</sub> nodes, despite controlling for zAUDIT scores;  $F(1,132) = 7.92$ ,  $p = .006$ ,  $\eta_p^2 = .057$ .

A partial correlation confirmed the direction of this interaction effect, by demonstrating that greater zCUDIT scores were related to weaker Early compared to Late Phase (Early – Late) functional connectivity while controlling for zAUDIT,  $r_{X|Y} = -.238$ ,  $p = .006$ . None of the 22 covariates altered the significance of the Experience Phase  $\times$  zCUDIT interaction effect on functional connectivity strength between RS<sub>Striatum</sub> and RS<sub>FP</sub> nodes (Effect Range:  $\eta_p^2 = .041 - .095$ ,  $p = <.001 - .020$ ). Also consistent with Group-level results, we failed to observe a significant interaction between Experience Phase  $\times$  zAUDIT scores on functional connectivity strength between RS<sub>Striatum</sub> and RS<sub>FP</sub> nodes,  $F(1,132) = 1.14$ ,  $p = .287$ ,  $\eta_p^2 = .009$ .

## Discussion

This study examined experience-related changes in adolescents' instrumental choice errors and functional connectivity among reward-sensitive striatal and frontoparietal regions. In support of our prediction, AUD<sub>High</sub> and CUD<sub>High</sub> groups exhibited significantly slower declines (i.e., decay rate) of instrumental choice error probabilities relative to the AUD-CUD<sub>Low</sub> group. These findings were comparable to those observed in adult alcohol use disorder,<sup>17</sup> and evidenced that adolescents with significant alcohol- and cannabis-use-disorder symptoms were slower to learn instrumental contingencies than adolescents without these symptoms. The AUD<sub>High</sub> group additionally exhibited significantly increased average choice error probabilities relative to AUD-CUD<sub>Low</sub> adolescents, whereas comparable effects were not observed for the CUD<sub>High</sub> group. These findings were consistent with a previous study examining continuous effects of adolescent AUD and CUD symptoms on instrumental choice performance<sup>4</sup> and intimate that AUD-related deficits in instrumental learning extend beyond slowed acquisition of instrumental contingencies.<sup>14,37</sup>

In support of our prediction for AUD-CUD<sub>Low</sub> adolescents, results showed that connectivity strength among reward-sensitive striatal and frontoparietal regions was strongest during the early phase of the PAT, wherein these adolescents exhibited a steep, experience-related decline in instrumental choice errors. During the late phase of the PAT, wherein these errors had a shallower decline, a significant reduction in functional connectivity strength

was observed between reward-sensitive striatal and frontoparietal regions. The coinciding experience-related changes observed for instrumental choice errors and connectivity strength correspond with hypotheses regarding the role of coordinated activation among the broader basal ganglia and task-relevant cortical areas during learning.<sup>20</sup> During the initial learning of instrumental contingencies, dopamine-related RPEs are posited to induce or enhance coordinated activation among basal ganglia and, task-relevant prefrontal and posterior cortical regions (e.g., parietal cortex). Once instrumental contingencies are sufficiently learned, instrumental errors and RPEs should approximate a local minimum<sup>8</sup>; concomitantly, coordinated activation among basal ganglia and these cortical regions should also be reduced.

Relatedly, we predicted that slower learning of instrumental contingencies for adolescents in the AUD<sub>High</sub> and CUD<sub>High</sub> groups would coincide with a relative delay in peak striatal-frontoparietal connectivity strength. Results supported this prediction for the CUD<sub>High</sub>, but not AUD<sub>High</sub> group. Compared to AUD-CUD<sub>Low</sub> adolescents, the CUD<sub>High</sub> group exhibited both a slower decay in choice errors and a later peak in their connectivity strength among reward-sensitive striatal and frontoparietal regions. The group by experience-phase interaction effect on functional connectivity among these regions retained significance despite covarying for AUD symptoms, as well as other potential confounds (e.g., psychiatric disorders). This effect also retained significance despite covarying for average activation in reward-sensitive striatal and frontoparietal regions and experience-related changes in striatal connectivity strength with other reward-sensitive regions. Together, these findings newly demonstrated a relative delay in peak functional connectivity strength: (1) coinciding with slowed instrumental learning; (2) specific to adolescent cannabis use; and (3) localized within striatal-frontoparietal connections.

The precise mechanisms influencing slower learning and a putative delay in coordinated activity among striatal and frontoparietal regions in CUD<sub>High</sub> adolescents are unclear. On one hand, these findings could relate to alterations in the ability of ascending (i.e., bottom-up) dopaminergic signals to modulate striatal and cortical regions. For instance, cannabis use is linked to diminished release of striatal dopamine during amphetamine challenge<sup>38</sup> and, decreased metabolic responses within the striatum and diffuse cortical regions during methylphenidate challenge<sup>39</sup>—suggesting a cannabis-use-related “blunting” of striatal and cortical responsiveness to dopamine.<sup>40</sup> On another hand, adolescent cannabis use has also been linked to altered activation in lateral prefrontal and parietal regions across various fMRI paradigms,<sup>41</sup> as well as deficits in cognitive processes supported by these regions (e.g., goal-directed attention)<sup>42</sup>. Thus, attention deficits or alterations to descending, top-down signaling processes might have also contributed to the present results. It is also possible that cannabis-related deficits in instrumental learning and delayed coordinated activation among striatal-cortical regions emerge from dysfunction within the recurrent interactions between striatal and frontoparietal regions, and the bottom-up and top-down processes these regions support.<sup>43</sup> Indeed, cannabis use disorder is also linked to reduced fractional anisotropy within striatal, peri-striatal, and cortical association (i.e., superior longitudinal fasciculi) white matter fibers<sup>44</sup>—suggesting the potential for inefficient or otherwise altered information transmission throughout striatal-frontoparietal structural circuits. Clearly, future research is needed to determine whether these or other mechanisms

give rise to the slowed learning and relatively delayed increases in striatal-frontoparietal connectivity strength associated with adolescent cannabis use.

We failed to observe significant experience-related changes within the AUD<sub>High</sub> group's striatal-frontoparietal connectivity. Bayesian analyses indicated that these findings were approximately 4.6 times more likely to have occurred under the null hypothesis (i.e., no experience-related change) compared to the alternative hypothesis (i.e., an experience-related change), evidencing *moderate* support<sup>45</sup> for the null hypothesis in the AUD<sub>High</sub> group (see Supporting Information). One explanation for these findings relates to greater impairments in instrumental learning and a general depression of the striatal-frontoparietal functions that support it for the AUD<sub>High</sub> group. This explanation was partially supported by our observation that the AUD<sub>High</sub>, but not the CUD<sub>High</sub> group, demonstrated increased probabilities of choice errors relative to the AUD-CUD<sub>Low</sub> group. Indeed, like the AUD<sub>High</sub> effects observed here, one study of typical adults demonstrated that fewer dynamic changes in striatal-cortical functional connections during learning were also related to increased probabilities of producing instrumental choice errors.<sup>18</sup> Although comparable findings are not available in adolescent substance use disorders, imaging studies contrasting adolescent AUD and CUD symptoms do demonstrate AUD-specific reductions of striatal and frontoparietal functions during instrumental learning.<sup>3,4</sup> For instance, in the same sample used here, increased AUD symptoms were related to reduced differentiation between reward and punishment feedback by activations within striatal and parietal regions.<sup>3</sup> In a separate sample and a different instrumental task, increased adolescent AUD symptoms were also shown to be related to reduced modulation of striatal, dlPFC, and parietal regions by RPEs.<sup>4</sup> Effects from both studies were observed despite controlling for CUD symptoms. In the context of the present and extant findings, we speculate that while adolescent CUD is characterized by slowed instrumental learning and relatively delayed increases in functional connectivity strength between brain regions supporting this learning; adolescent AUD may be better characterized in relation to a broader impairment in instrumental learning and a more general functional depression of the striatal-frontoparietal systems that support it. Although this speculation requires additional confirmation, it underscores an intriguing possibility for distinct behavioral and neural phenomena differentially characterizing instrumental, or potentially broader reinforcement learning, in the two most prevalent adolescent substance use disorders.

### Limitations and Future Directions

The present results should be considered in the context of several limitations. First, although 94% of adolescents within the AUD<sub>High</sub> and CUD<sub>High</sub> groups were residents of a supervised treatment facility and subject to random drug screening for at least four weeks prior to scanning, biological confirmation of abstinence was not available the day of scanning. Second, following adolescent epidemiological trends,<sup>46</sup> alcohol and cannabis co-use was high in the present sample. While the use of AUDIT and CUDIT dimensional covariates provided support for the specificity of our functional connectivity effects, participant-overlap precluded AUD<sub>High</sub> and CUD<sub>High</sub> group comparisons. Future work should consider directly contrasting single- and co-use groups to disentangle substance-use-disorder effects more definitively. Third, although we examined the impact of 22 covariates

on significant functional connectivity effects, covariate interactions were not examined. Fourth, AUDIT and CUDIT scores assayed recent substance-use-disorder symptoms, however, comprehensive substance-use histories (e.g., age of first use, duration of use) were not available. As these histories have been shown to relate to altered striatal-frontoparietal, resting-state functional connectivity,<sup>47</sup> future research is warranted to evaluate the influence of such factors on functional connectivity during instrumental learning. Finally, given the paucity of studies examining task-based functional connectivity related to adolescent alcohol or cannabis use, future research should examine the extent to which the present findings generalize to the broader population.

## Conclusions

Adolescents with significant alcohol- or cannabis-use-disorder symptoms learned instrumental contingencies slower than adolescents without these symptoms. In adolescents without significant alcohol- or cannabis-use-disorder symptoms, their relatively fast learning coincided with stronger functional connectivity between striatal and frontoparietal regions early during experience with instrumental cues relative to later. For adolescents with significant cannabis-use-disorder symptoms, their relatively slow learning coincided with stronger striatal-frontoparietal connectivity during later experience relative to earlier. Adolescents with significant alcohol-use-disorder symptoms failed to exhibit significant changes in striatal-frontoparietal connectivity strength across experience phases, which may have related to a reduced overall capacity for instrumental learning and a general depression of the striatal and frontoparietal functions that support it. Research is needed to realize the translational potential of the present findings. However, because several therapies for substance use disorders rely upon learning novel instrumental associations,<sup>12</sup> an understanding of specific substance-related limitations in this learning and dysfunctions in associated neural circuits may prove fruitful for optimizing these or related treatments for adolescent alcohol- or cannabis-use disorders.

## Supplementary Material

Refer to Web version on PubMed Central for supplementary material.

## Acknowledgements:

The authors wish to thank Jeffrey Stevens for helpful consultation on the manuscript. NAH was partially supported by the Brain and Behavior Research Foundation. NAH and KTW were partially supported by the Nebraska Biomedical Research Development Funds. NAH, KTW, and RJRB were partially supported by the Rural Drug Addiction Research Center (P20GM130461). The content of this report is solely the responsibility of the authors and does not necessarily represent the official views of the National Institutes of Health or of any other sponsor.

## References

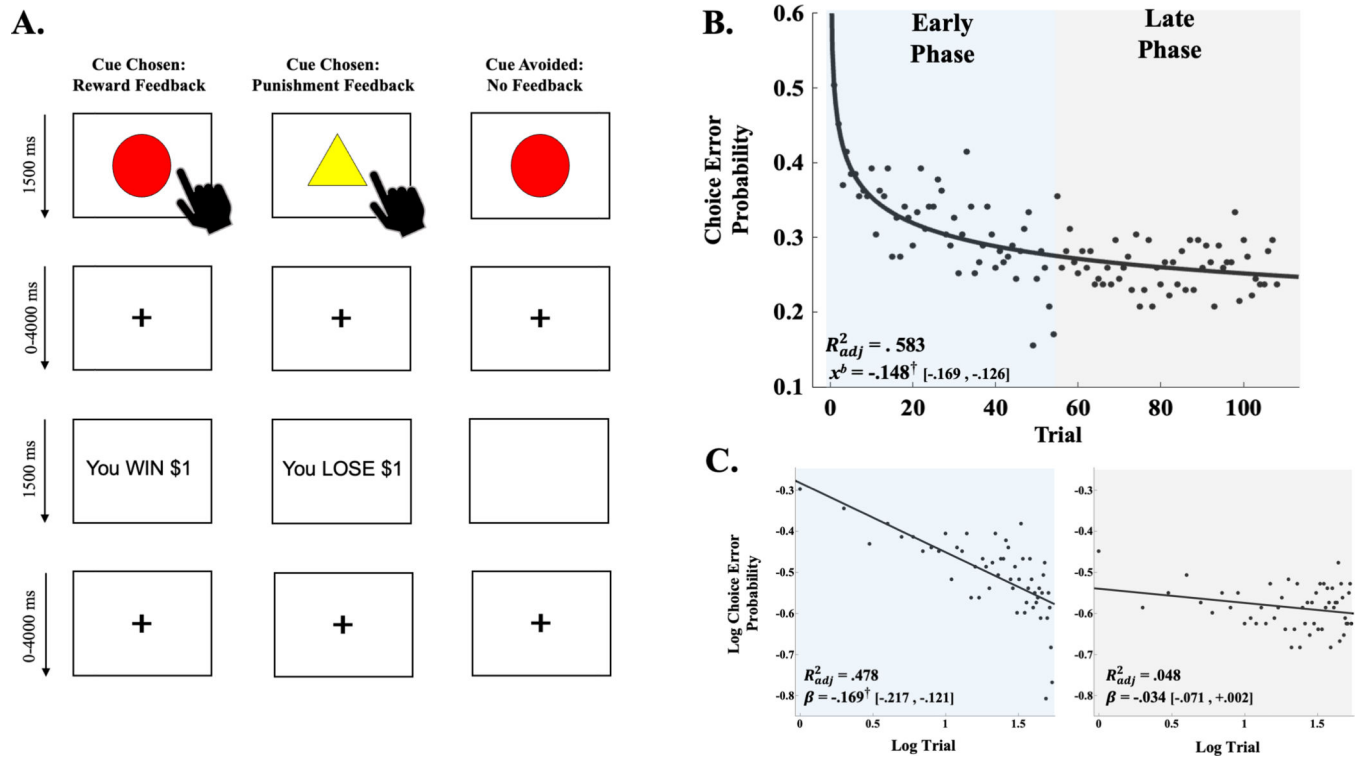
1. Substance Abuse and Mental Health Services Administration (2017): Results from the 2016 National Survey on Drug Use and Health: Detailed tables. Available at: <https://www.samhsa.gov/data/report/results-2016-national-survey-drug-use-and-health-detailed-tables>. Accessed March 8, 2021.
2. Aloï J, Meffert H, White SF, et al. Differential dysfunctions related to alcohol and cannabis use disorder symptoms in reward and error-processing neuro-circuitries in adolescents. *Dev Cogn Neurosci*. 2019;36(January). doi:10.1016/j.dcn.2019.100618

3. Aloï J, Blair KS, Crum KI, et al. Alcohol Use Disorder, But Not Cannabis Use Disorder, Symptomatology in Adolescents Is Associated With Reduced Differential Responsiveness to Reward Versus Punishment Feedback During Instrumental Learning. *Biol Psychiatry Cogn Neurosci Neuroimaging*. 2020;5(6):610–618. doi:10.1016/j.bpsc.2020.02.003 [PubMed: 32299790]
4. Aloï J, Crum KI, Blair KS, et al. Individual associations of adolescent alcohol use disorder versus cannabis use disorder symptoms in neural prediction error signaling and the response to novelty. *Dev Cogn Neurosci*. 2021;48(April):100944. doi:10.1016/j.dcn.2021.100944
5. Jager G, Block RI, Luijten M, Ramsey NF. Tentative Evidence for Striatal Hyperactivity in Adolescent Cannabis-Using Boys: A Cross-Sectional Multicenter fMRI Study. *J Psychoactive Drugs*. 2013;45(2):156–167. doi:10.1080/02791072.2013.785837 [PubMed: 23909003]
6. Whelan R, Watts R, Orr CA, et al. Neuropsychosocial profiles of current and future adolescent alcohol misusers. *Nature*. 2014;512(7513):185–189. doi:10.1038/nature13402 [PubMed: 25043041]
7. O’Doherty J, Dayan P, Schultz J, Deichmann R, Friston K, Dolan RJ. Dissociable Roles of Ventral and Dorsal Striatum in Instrumental Conditioning. *Science* (80- ). 2004;304(5669):452–454. doi:10.1126/science.1094285
8. Schultz W. Neuronal reward and decision signals: From theories to data. *Physiol Rev*. 2015;95(3):853–951. doi:10.1152/physrev.00023.2014 [PubMed: 26109341]
9. Everitt BJ, Robbins TW. Drug addiction: Updating actions to habits to compulsions ten years on. *Annu Rev Psychol*. 2016;67:23–50. doi:10.1146/annurev-psych-122414-033457 [PubMed: 26253543]
10. Keiflin R, Janak PH. Dopamine Prediction Errors in Reward Learning and Addiction: From Theory to Neural Circuitry. *Neuron*. 2015;88(2):247–263. doi:10.1016/j.neuron.2015.08.037 [PubMed: 26494275]
11. Koob GF, Volkow ND. Neurobiology of addiction: a neurocircuitry analysis. *The Lancet Psychiatry*. 2016;3(8):760–773. doi:10.1016/S2215-0366(16)00104-8 [PubMed: 27475769]
12. Moos RH. Theory-based active ingredients of effective treatments for substance use disorders. *Drug Alcohol Depend*. 2007;88(2–3):109–121. doi:10.1016/j.drugalcdep.2006.10.010 [PubMed: 17129682]
13. O’Doherty JP, Cockburn J, Pauli WM. Learning, Reward, and Decision Making. *Annu Rev Psychol*. 2017;68:73–100. doi:10.1146/annurev-psych-010416-044216 [PubMed: 27687119]
14. Malone SM, Luciana M, Wilson S, et al. Adolescent drinking and motivated decision-making: A cotwin-control investigation with monozygotic twins. *Behav Genet*. 2014;44(4):407–418. doi:10.1007/s10519-014-9651-0 [PubMed: 24676464]
15. White SF, Tyler P, Botkin ML, et al. Youth with substance abuse histories exhibit dysfunctional representation of expected value during a passive avoidance task. *Psychiatry Res - Neuroimaging*. 2016;257(August):17–24. doi:10.1016/j.psychresns.2016.08.010 [PubMed: 27716545]
16. Tolomeo S, Yaple ZA, Yu R. Neural representation of prediction error signals in substance users. *Addiction Biology*. 2021;26:e12976
17. Park SQ, Kahnt T, Beck A, et al. Prefrontal cortex fails to learn from reward prediction errors in alcohol dependence. *J Neurosci*. 2010;30(22):7749–7753. doi:10.1523/JNEUROSCI.5587-09.2010 [PubMed: 20519550]
18. Gerraty RT, Davidow JY, Foerde K, Galvan A, Bassett DS, Shohamy D. Dynamic flexibility in striatal-cortical circuits supports reinforcement learning. *J Neurosci*. 2018;38(10):2442–2453. doi:10.1523/JNEUROSCI.2084-17.2018 [PubMed: 29431652]
19. Li J, Delgado MR, Phelps EA. How instructed knowledge modulates the neural systems of reward learning. *Proc Natl Acad Sci U S A*. 2011;108(1):55–60. doi:10.1073/pnas.1014938108 [PubMed: 21173266]
20. Hélie S, Ell SW, Ashby FG. Learning robust cortico-cortical associations with the basal ganglia: An integrative review. *Cortex*. 2015;64(October):123–135. doi:10.1016/j.cortex.2014.10.011 [PubMed: 25461713]
21. Aloï J, Blair KS, Crum KI, et al. Adolescents show differential dysfunctions related to Alcohol and Cannabis Use Disorder severity in emotion and executive attention neuro-circuitries. *NeuroImage Clin*. 2018;19(January):782–792. doi:10.1016/j.nicl.2018.06.005 [PubMed: 29988822]

22. Wechsler D. Wechsler abbreviated scale of intelligence- 2 ed. San Antonio, TX: NCS Pearson; 2011.
23. World Health Organization. AUDIT: The alcohol use disorders identification test: Guidelines for use in primary health care. World Health Organization, 2001
24. Adamson SJ, Sellman JD. A prototype screening instrument for cannabis use disorder: The Cannabis Use Disorders Identification Test (CUDIT) in an alcohol-dependent clinical sample. *Drug Alcohol Rev.* 2003;22(3):309–315. doi:10.1080/0959523031000154454 [PubMed: 15385225]
25. Fairlie AM, Sindelar HA, Eaton CA, Spirito A. Utility of the AUDIT for screening adolescents for problematic alcohol use in the emergency department. *Int. J. Adolesc. Med. Health* 18, 115–122. doi:10.1515/IJAMH.2006.18.1.115
26. Esteban O, Markiewicz CJ, Blair RW, et al. fMRIPrep: a robust preprocessing pipeline for functional MRI. *Nat Methods.* 2019;16(1):111–116. doi:10.1038/s41592-018-0235-4 [PubMed: 30532080]
27. Hubbard NA, Romeo RR, Grotzinger H, et al. Reward-sensitive basal ganglia stabilize the maintenance of goal-relevant neural patterns in adolescents. *J Cogn Neurosci.* 2020;32(8):1508–1524. doi:10.1162/jocn\_a\_01572 [PubMed: 32379000]
28. Hubbard NA, Auerbach RP, Siless V, et al. Connectivity patterns evoked by fearful faces demonstrate reduced flexibility across a shared dimension of adolescent anxiety and depression. *Clinical Psychological Science.* April 2022. doi:10.1177/21677026221079628
29. Simmonds DJ, Hallquist MN, Luna B. Protracted development of executive and mnemonic brain systems underlying working memory in adolescence: A longitudinal fMRI study. *Neuroimage.* 2017;157(June 2016):695–704. doi:10.1016/j.neuroimage.2017.01.016
30. Power JD, Barnes KA, Snyder AZ, Schlaggar BL, Petersen SE. Spurious but systematic correlations in functional connectivity MRI networks arise from subject motion. *Neuroimage.* 2012;59(3):2142–2154. doi:10.1016/j.neuroimage.2011.10.018 [PubMed: 22019881]
31. Cox RW. AFNI: Software for analysis and visualization of functional magnetic resonance neuroimages. *Comput Biomed Res.* 1996;29(29):162–173. [https://ac-els-cdn-com.ezp-prod1.hul.harvard.edu/S0010480996900142/1-s2.0-S0010480996900142-main.pdf?\\_tid=c22bae7a-b8f5-4a8b-9dac-91c1ed841d53&acdnt=1549393398\\_e37181b8933a2ac88c2d7dc0eab14413](https://ac-els-cdn-com.ezp-prod1.hul.harvard.edu/S0010480996900142/1-s2.0-S0010480996900142-main.pdf?_tid=c22bae7a-b8f5-4a8b-9dac-91c1ed841d53&acdnt=1549393398_e37181b8933a2ac88c2d7dc0eab14413) [PubMed: 8812068]
32. Rissman J, Gazzaley A, D’Esposito M. Measuring functional connectivity during distinct stages of a cognitive task. *Neuroimage.* 2004;23(2):752–763. doi:10.1016/j.neuroimage.2004.06.035 [PubMed: 15488425]
33. Rubinov M, Sporns O. Complex network measures of brain connectivity: Uses and interpretations. *Neuroimage.* 2010;52(3):1059–1069. doi:10.1016/j.neuroimage.2009.10.003 [PubMed: 19819337]
34. Glautier S. Revisiting the learning curve (once again). *Front Psychol.* 2013;4(DEC):1–17. doi:10.3389/fpsyg.2013.00982 [PubMed: 23382719]
35. Pavlik PI, Anderson JR. Practice and forgetting effects on vocabulary memory: An activation-based model of the spacing effect. *Cogn Sci.* 2005;29(4):559–586. doi:10.1207/s15516709cog0000\_14 [PubMed: 21702785]
36. Miech RA, Johnston LD, O’Malley PM, Bachman JG, Schulenberg JE. Monitoring the Future national survey results on drug use, 1975–2015: Volume I, secondary school students. University of Michigan, Institute for Social Research. Available at: <https://files.eric.ed.gov/fulltext/ED578604.pdf>
37. Xiao L, Bechara A, Gong Q, et al. Abnormal affective decision making revealed in adolescent binge drinkers using a functional magnetic resonance imaging study. *Psychol Addict Behav.* 2013;27(2):443–454. doi:10.1037/a0027892 [PubMed: 22486330]
38. van de Giessen E, Weinstein JJ, Cassidy CM, et al. Deficits in striatal dopamine release in cannabis dependence. *Mol Psychiatry.* 2017;22(1):68–75. doi:10.1038/mp.2016.21 [PubMed: 27001613]
39. Wiers CE, Shokri-Kojori E, Wong CT, et al. Cannabis abusers show hypofrontality and blunted brain responses to a stimulant challenge in females but not in males. *Neuropsychopharmacology.* 2016;41(10):2596–2605. doi:10.1038/npp.2016.67 [PubMed: 27156854]

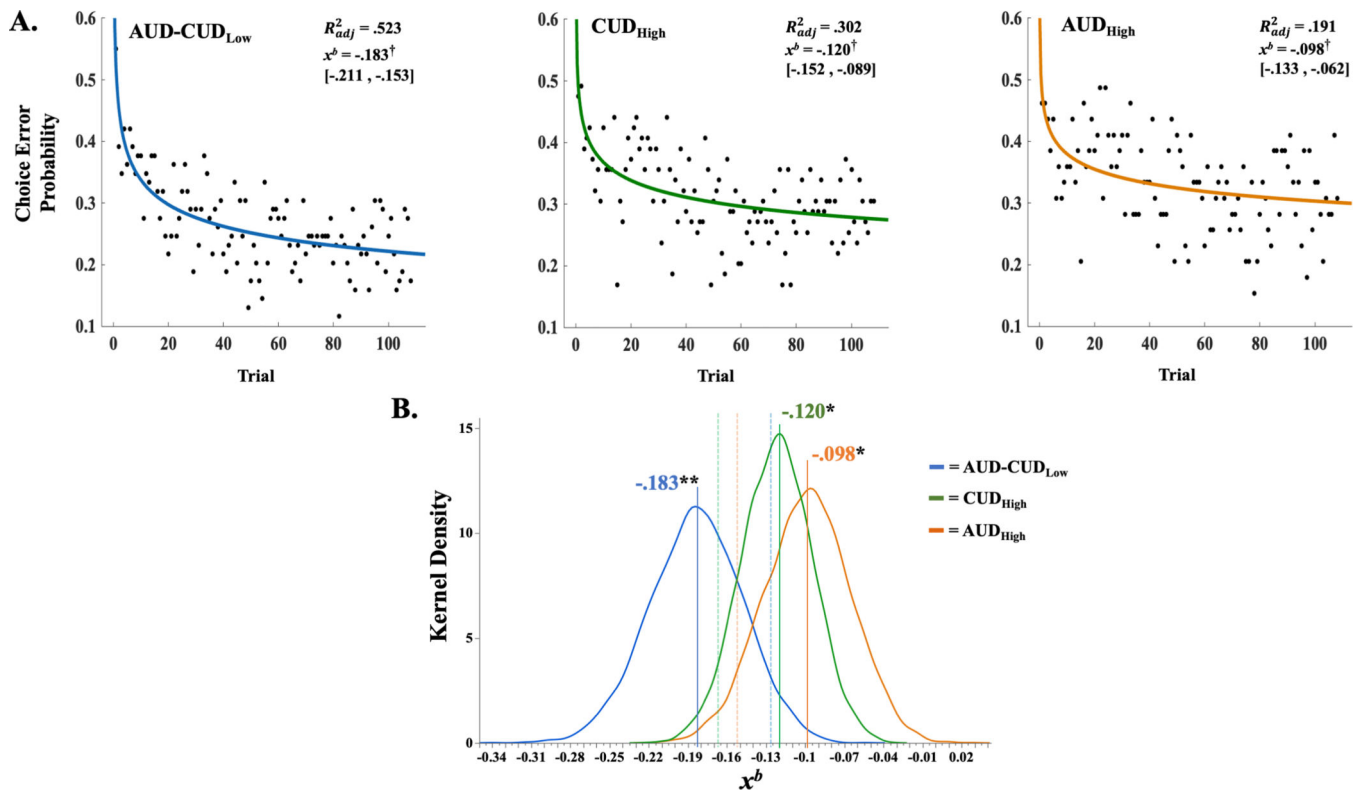
40. Bloomfield MAP, Ashok AH, Volkow ND, Howes OD. The effects of  $\delta$ 9-tetrahydrocannabinol on the dopamine system. *Nature*. 2016;539(7629):369–377. doi:10.1038/nature20153 [PubMed: 27853201]
41. Blest-Hopley G, Giampietro V, Bhattacharyya S. Regular cannabis use is associated with altered activation of central executive and default mode networks even after prolonged abstinence in adolescent users: Results from a complementary meta-analysis. *Neurosci Biobehav Rev*. 2019;96(October 2018):45–55. doi:10.1016/j.neubiorev.2018.10.026 [PubMed: 30395923]
42. Broyd SJ, Van Hell HH, Beale C, Yücel M, Solowij N. Acute and chronic effects of cannabinoids on human cognition - A systematic review. *Biol Psychiatry*. 2016;79(7):557–567. doi:10.1016/j.biopsych.2015.12.002 [PubMed: 26858214]
43. Radulescu A, Niv Y, Ballard I. Holistic Reinforcement Learning: The role of structure and attention. *Trends Cogn Sci*. 2019;23(4):278–292. doi:10.1016/j.tics.2019.01.010 [PubMed: 30824227]
44. Manza P, Yuan K, Shokri-Kojori E, Tomasi D, Volkow ND. Brain structural changes in cannabis dependence: association with MAGL. *Mol Psychiatry*. 2020;25(12):3256–3266. doi:10.1038/s41380-019-0577-z [PubMed: 31695165]
45. Jeffreys H *Theory of probability*. 3<sup>rd</sup> ed. Oxford University Press. 1961.
46. Mason WA, Chmelka MB, Howard BK, Thompson RW. Comorbid alcohol and cannabis use disorders among high-risk youth at intake into residential care. *J Adolesc Heal*. 2013;53(3):350–355. doi:10.1016/j.jadohealth.2013.04.002
47. Weissman DG, Schriber RA, Fassbender C, et al. Earlier adolescent substance use onset predicts stronger connectivity between reward and cognitive control brain networks. *Dev Cogn Neurosci*. 2015;16:121–129. doi:10.1016/j.dcn.2015.07.002 [PubMed: 26215473]
48. Talairach J, Tournoux P. *Co-planar Stereotactic Atlas of the Human Brain. 3-D proportioned system: an approach to cerebral imaging*. Stuttgart: G Thieme, 1988.
49. Fan L, Li H, Zhuo J, et al. The Human Brainnetome Atlas: A New Brain Atlas Based on Connectional Architecture. *Cereb Cortex*. 2016;26(8):3508–3526. doi:10.1093/cercor/bhw157 [PubMed: 27230218]
50. Eickhoff SB, Stephan KE, Mohlberg H, et al. A new SPM toolbox for combining probabilistic cytoarchitectonic maps and functional imaging data. *Neuroimage*. 2005;25(4):1325–1335. doi:10.1016/j.neuroimage.2004.12.034 [PubMed: 15850749]





**Figure 1.**

(A) Illustration of reward, punishment and no-feedback scenarios of passive avoidance task (PAT). (B) Power-series regression curve of choice error probability computed across entire sample for operationalized early- and late-experience phases. Adjusted coefficient of determination ( $R_{adj}^2$ ) and decay coefficient ( $x^b$ ) derived from power-series regression model. Brackets contain parametric, 95% confidence limits of  $x^b$ . Colour shading illustrates operationalization of early- and late-experience phases. (C) Linear regression curves for log choice error probabilities from early (blue) and late (grey) phase trials.  $R_{adj}^2$  and regression slope estimates ( $\beta$ ) derived from linear regressions fit to log trial by log choice error probability. Brackets contain parametric, 95% confidence limits of  $\beta$ . † denotes parametric, 95% confidence interval of  $x^b$  coefficient (B) or log-log regression  $\beta$  (C) did not contain 0. Panel A adapted from Aloï and colleagues<sup>3</sup>

**Figure 2.**

(A) Power-series regression curves and model fit estimates by group across passive avoidance task (PAT) trials. Adjusted coefficient of determination ( $R_{adj}^2$ ) and decay-rate coefficient ( $x^b$ ) derived from each group's power-series regression model. Brackets contain parametric, 95% confidence limits of  $x^b$ . (B) Smoothed frequency distributions (kernel density) of  $x^b$  coefficient derived from bootstrapped-resampling procedure for adolescents meeting the criteria for significant cannabis (CUD<sub>High</sub> [green]) or alcohol use disorder symptoms (AUD<sub>High</sub> [orange]), compared with adolescents not meeting these criteria (AUD-CUD<sub>Low</sub> [blue]). Solid vertical lines and associated text reflect parametric  $x^b$  derived from each group's power-series regression. Dashed vertical lines reflect 95th percentile limits of bootstrap distribution. † denotes parametric, 95% confidence interval of  $x^b$  did not contain 0. \* denotes CUD<sub>High</sub> or AUD<sub>High</sub> group's parametric  $x^b$  did not surpass the upper bound of the AUD-CUD<sub>Low</sub> group's 95% confidence limit (95% UCL = -.126). \*\* denotes AUD-CUD<sub>Low</sub> group's parametric  $x^b$  did not surpass the lower bound of the CUD<sub>High</sub> (95% LCL = -.167) or AUD<sub>High</sub> (95% LCL = -.153) 95% confidence limits

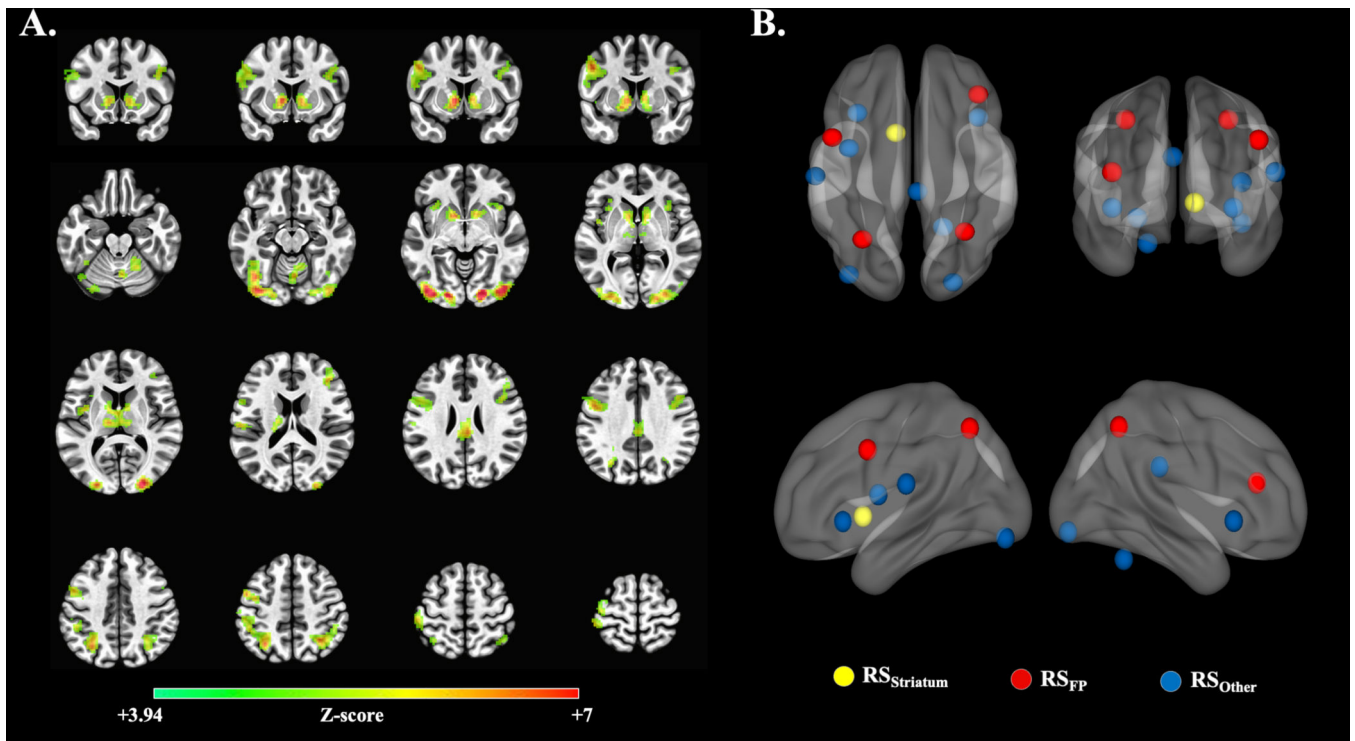


**Figure 3.** (A) Sample-wide, voxel clusters exhibiting significant activation during high-reward probability cues relative to high-punishment probability cues ( $\text{High}_{\text{Reward}} > \text{High}_{\text{Punish}}$  activation;  $z = 3.94$ ;  $k$ -faces-touching voxels  $> 49$ ;  $\text{FWER}$ -corrected  $p < 0.001$ ). (B) Illustration of the 13 non-overlapping reward-sensitive nodes. Colours reflect reward-sensitive node grouping. See Table 2 for anatomical and node labels, as well as LPI coordinates.

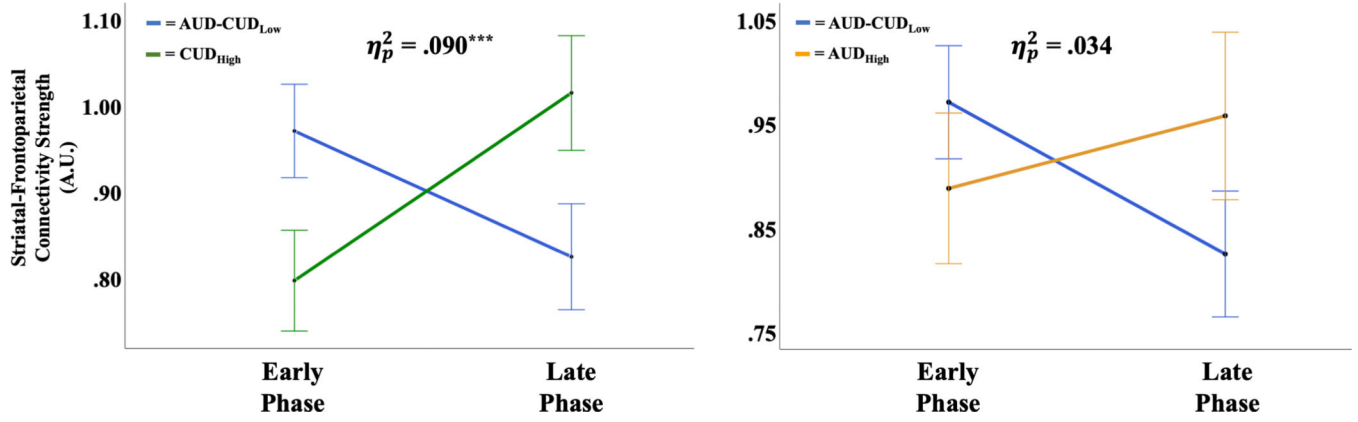


**Figure 4.** Striatal–frontoparietal marginal mean functional connectivity strength by substance use dependence group. Error bars reflect 1 standard error of the mean.  $\eta_p^2$ , partial eta-squared group by experience phase effect size. \*\*\* denotes  $p < 0.001$ .

**Table 1.**

Quality Assured Sample Characteristics by Substance-use-disorder Group (N = 135)

	AUD <sub>High</sub>	CUD <sub>High</sub>	AUD-CUD <sub>Low</sub>
<i>N</i> <sup>a</sup>	39	59	69
<b>Percent Male</b>	56.4	66.1	59.4
<b>Percent In-patient</b>	92.3 *	94.9 *	55.1
<b>Mean Age (SEM)</b>	16.9 (.16) *	16.5 (.13) *	16.5 (.14)
<b>Mean AUDIT (SEM)</b>	10.2 (1.2) *	06.5 (.96) *	00.5 (.10)
<b>Mean CUDIT (SEM)</b>	16.2 (1.3) *	17.7 (.88) *	01.1 (0.3)
<b>Median Smoking (MAD)</b>	03.0 (0.5) *	03.0 (1.0) *	00.5 (0.1)
<b>Mean FS-IQ (SEM)</b>	99.7 (1.8)	100.1 (1.4)	99.5 (1.2)
<b>Mean FD (SEM)</b>	0.14 (.01)	0.13 (.01)	0.14 (.01)
<b>Mean Censored (SEM)</b>	2.95 (.65)	2.51 (.49)	2.13 (.44)
<b>Percent Psych. Med.</b>			
Any	41.0	39.0	24.6
Antidepressant	33.3 *	28.9 *	08.7
Stimulant	12.8	15.3	15.9
Other	05.1	08.5	11.6
<b>Percent DSM-5 Diagnosis</b>			
Any	94.9 *	94.9 *	50.7
ADHD	66.7 *	69.5 *	34.8
Conduct Disorder	69.2 *	69.5 *	23.2
Generalized Anxiety	48.7 *	39.0 *	15.9
Major Depression	25.6	22.0	11.6
ODD	71.8 *	78.0 *	33.3
PTSD	25.6 *	16.9	07.2
Social Anxiety	35.9 *	25.4	13.0

AUD<sub>High</sub> = significant alcohol-use-disorder symptom status; CUD<sub>High</sub> = significant cannabis-use-disorder symptom status; AUD-CUD<sub>Low</sub> = clinical threshold not met for AUD nor CUD; AUDIT = Alcohol Use Disorder Identification Test; CUDIT = Cannabis Use Disorder Identification Test; SEM = 1 standard error of mean; Smoking = cigarette use (0 [never] to 4 [current, regular use]) reported on Monitoring the Future Survey<sup>36</sup>; MAD = median absolute deviation; FS-IQ = full-scale intelligence quotient obtained from Weschler Abbreviated Scale of Intelligence<sup>22</sup>; FD = average framewise displacement after motion censoring; Censored = mean number of motion-censored frames; Other = non-stimulant attention deficit hyperactivity disorder medication, antipsychotic, or mood-stabilizer. ADHD = attention deficit hyperactivity disorder; ODD = oppositional defiant disorder; PTSD = post-traumatic stress disorder.

\* = significant group difference between substance-use group and AUD-CUD<sub>Low</sub>. For AUD<sub>High</sub> and CUD<sub>High</sub> between-groups statistical comparisons to AUD-CUD<sub>Low</sub> see Supporting Information Tables 1–2.

<sup>a</sup>Note: AUD<sub>High</sub> and CUD<sub>High</sub> groups were not exclusive and could include participants meet threshold for AUD<sub>High</sub> and/or CUD<sub>High</sub>.

**Table 2.**

## Reward-sensitive Nodes, Anatomical Labels, and Coordinates

Anatomical Label (BAs)	X	Y	Z	Voxels	Node Group
L Ventral Caudate	-10	08	00	587	RS <sub>Striatum</sub>
L Superior Parietal Lobule (7)	-30	-61	49	809	RS <sub>FP</sub>
L Inferior Frontal Gyrus (9,6,8)	-48	05	36	366	RS <sub>FP</sub>
R Inferior Parietal Lobule (7,40)	31	-56	49	286	RS <sub>FP</sub>
R Middle Frontal Gyrus (46,10)	39	33	18	256	RS <sub>FP</sub>
L Inferior Occipital Gyrus (19,18)	-38	-84	-12	806	RS <sub>Other</sub>
R Lingual Gyrus (18,17)	23	-89	-09	714	RS <sub>Other</sub>
R Lobule VI	18	-53	-24	280	RS <sub>Other</sub>
Cingulate Gyrus (23,31)	03	-30	27	182	RS <sub>Other</sub>
L Postcentral Gyrus (40,41,42)	-58	-20	18	078	RS <sub>Other</sub>
L Insula (13,44)	-38	-02	12	070	RS <sub>Other</sub>
R Inferior Frontal Gyrus/Insula (47,13)	-33	21	-03	067	RS <sub>Other</sub>
L Inferior Frontal Gyrus/Insula (47,13)	39	18	-03	067	RS <sub>Other</sub>

Anatomical labels and coordinates reflect peak voxels within significant cluster in MNI space. Lateral distinctions are not made within 5 mm of midline. Significance evaluated at  $z = 3.94$ ;  $k$ -faces-touching voxels  $> 49$ ;  $FWER$ -corrected  $p < .001$ . Brodmann's Areas (BAs) within 5 mm of cluster peak voxel are listed in order of proximity for gyrus labels. Gyrus labels based upon Talairach-Tournoux atlas.<sup>48</sup> Subcortical labels based Brainnetome 1.0 Atlas.<sup>49</sup> Cerebellar labels derived from Eickhoff-Zilles cytoarchitectonic atlas.<sup>50</sup> RS<sub>FP</sub> = reward-sensitive frontoparietal node. RS<sub>Striatum</sub> = reward-sensitive striatal node. RS<sub>Other</sub> = reward-sensitive nodes not within striatum nor frontoparietal regions. *Note:* Data were extracted from these original cluster peak voxel using a 7 mm sphere from which each network node had an equivalent voxel count ( $n_{VOX} = 73$ ).